Wind and Structures, Vol. 14, No. 3 (2011) 209-220
DOI: http://dx.doi.org/10.12989/was.2011.14.3.209

Investigation on the wind-induced instability of long-span suspension bridges with 3D cable system

Xin-Jun Zhang*

College of Civil Engineering and Architecture, Zhejiang University of Technology, Hangzhou 310032, P.R. China

(Received September 28, 2009, Accepted November 9, 2010)

Abstract. The cable system is generally considered to be a structural solution to increase the spanning capacity of suspension bridges. In this work, based on the Runyang Bridge over the Yangtze River, three case suspension bridges with different 3D cable systems are designed, structural dynamic characteristics, the aerostatic and aerodynamic stability are investigated numerically by 3D nonlinear aerostatic and aerodynamic analysis, and the cable system favorable to improve the wind-induced instability of long-span suspension bridges is also proposed. The results show that as compared to the example bridge with parallel cable system, the suspension bridge with inward-inclined cable system has greater lateral bending and tensional frequencies, and also better aerodynamic stability; as for the suspension bridge with outward-inclined cable system, it has less lateral bending and tensional frequencies, and but better aerostatic stability; however the suspension bridge is more prone to aerodynamic instability, and therefore considering the whole wind-induced instability, the parallel and inward-inclined cable systems are both favorable for long-span suspension bridges.

Keywords: long-span suspension bridge; 3D cable system; dynamic characteristics; aerostatic stability; aerodynamic stability.

1. Introduction

As the bridge span is greater than 1000 m, suspension bridge is generally believed to be the most favorable bridge structure. Currently, the common suspension bridges have two parallel main cables, which are defined as parallel cable system herein. Previous investigations show that the suspension bridge with parallel cable system is favorable to carry the vertical loads, and however it is weak in carrying the lateral loads such as the wind load(Astiz 1998, Gimsing 1997). By the end of the last century, the Akashi Kaikyo Bridge(1990 m) in Japan and the Great Belt Bridge(1624 m) in Denmark represent an outstanding engineering achievement in building suspension bridge with main span approaching 2000 m. In the 21st century, world's bridge construction is entering to a new era of building sea-crossing and island-linking bridges. To meet with the navigation requirement and avoid the construction of deep-water foundations, even longer span are being planned, such as the Messina bridge(3300 m) in Italy and the Gibraltar bridge between Spain and Morocco(3550 m) (Astiz 1998). However the required deck width does not increase with the bridge span, and the

* Corresponding Author, Professor, E-mail: xjzhang@zjut.edu.cn

width to span ratio of the deck consequently becomes less, which results in great reduction of the lateral bending and tensional stiffness, the lateral load capacity and also structural stability. How to increase the lateral bending and tensional stiffness and also structural stability becomes an important problem for the design of longer span suspension bridges. Fortunately, the 3D cable system has been confirmed to be effective in strengthening the lateral and tensional stiffness whilst remaining the vertical bending stiffness almost unchanged. In addition, with increasing of bridge span, the bending and tensional frequencies both decrease and tend to approach each other, and as a result the classical flutter occurs at a lower wind speed. However through adjusting the cable system, to a certain extent, the tensional and lateral bending motions become coupled, which is helpful to increase the tensional frequency and also the flutter stability of the bridge. Therefore, 3D cable system provides an effective structural solution for long and particular super long-span suspension bridge(Astiz 1998, Gimsing 1997, Jensen 2001, Xiang and Ge 2007). At present, 3D cable system is mainly used in several self-anchored suspension bridges with short span(Ochsendorf and Billington 1999). Though there is no practical application of 3D cable system in the earth-anchored suspension bridges, it is frequently proposed in a few of long and super long-span suspension bridges such as the Messina Bridge and the Gibraltar Bridge etc(Astiz 1998, Gimsing 1997, Larsen and Astiz 1998).

Up to now, more attentions were paid to the self-anchored suspension bridges with 3D cable system including the shape-finding analysis, the computational theory, construction, and the earthquake and wind resistance etc. (Luo 2004, *Zhou et al*. 2006, Kim *et al.* 2002, Kwon *et al.* 1995), but for the ground-anchored suspension bridges with 3D cable system, few investigations have been conducted. For the common self-anchored suspension bridges with short span, the wind-induced instability problem is not prominent. But for the common ground-anchored suspension bridges with main span over 1000 m, the wind-induced instability is believed generally to be a governing factor for their design. Currently, the wind-induced instability of common ground-anchored suspension bridges with parallel cable system is comprehensively investigated. As for the ground-anchored suspension bridge with 3D cable system, how the wind-induced instability varies needs to be further investigated. But until now, there are few investigations on the wind-induced instability of suspension bridge with 3D cable system(Astiz 1996, 1998, Osamu *et al.* 2004, Xiang and Ge 2007, Larsen and Astiz 1998, Kubo *et al.*1995).

To find out the favorable cable system for long-span suspension bridges, in this work, based on a long-span suspension bridge-the Runyang Bridge over the Yangtze River with main span of 1490 m, three case bridges with different 3D cable systems are designed, structural dynamic characteristics, the aerostatic and aerodynamic stability are investigated numerically by 3D nonlinear aerostatic and aerodynamic analysis, and the cable system favorable to improve the wind-induced instability of long-span suspension bridges is also discussed.

2. Description of the example and case bridges

2.1. The example bridge

The Runyang Bridge over the Yangtze River is the longest suspension bridge built in China, and has a 1490 m main span and two 470 m side spans, as shown in Fig. 1. The cable's sag to span ratio is 1/10, and the lateral interval of two main cables is 34.3 m, the standard interval of hangers

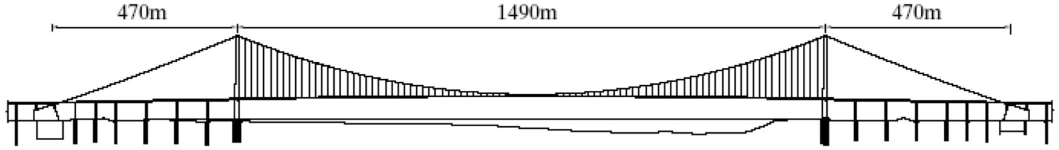

(a) Elevation

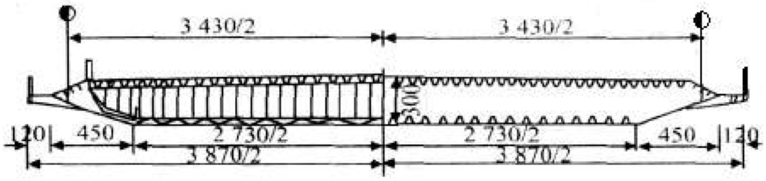

(b) Cross section of the bridge deck(Unit: mm)

Fig. 1 General layout of the Runyang Bridge over the Yangtze River

Table 1 The material and cross-sectional properties of the example bridge

Structural members	E/(Mpa)	A/m^2	J_d/m^4	I_y/m^4	I_z/m^4	M/(Kg/m)	J_m/(Kg.m^2/m)
Girder	2.1×10^5	1.2481	5.034	137.7541	1.9842	18386.5	1.852×10^6
Cable	2.0×10^5	0.47347	-	-	-	3817.4	-
Hanger	2.0×10^5	0.00214	-	-	-	16.8	-

Note: E-elastic modulus, A-Cross-sectional area, J_d-torsional moment of inertia, I_z-vertical bending moment of inertia, I_y-lateral bending moment of inertia, M-mass per unit length, J_m-mass moment of inertia per unit length.

is 16 m; the deck is a 3.0 m high and 38.7 m wide steel streamlined box girder. The towers are door-shaped frames with about 209 m high. The material and cross-sectional properties of the bridge are present in Table 1.

2.2. The case bridges with 3D cable systems

Based on the example bridge, three case bridges with different 3D cable systems are designed. Except the cable system and the towers, other structural parameters of the case bridges are remained the same as those of the example bridge, and they are described briefly as follows.

(1) Inward-inclined cable system 1. As shown in Fig. 2(b), the distance of two main cables is reduced to as narrow as possible at the tower top and is gradually expanded towards the midpoint of main span by the transverse component of the hangers' tension. The two towers are A-shaped frames as shown in Fig. 3(b), and their material and sectional properties are the same as those of the example bridge; the cable sag to span ratio is 1/10 in elevation, and 14.15/1490 in plane, the distance of two main cables at tower top is 6 m.

(2) Inward-inclined cable system 2. As shown in Fig. 2(c), based on the inward-inclined case bridge 1, the distance of two main cables at tower top increases to 17.15 m, which is one half of the cable distance of the example bridge at the tower top. The two towers are both trapezoid door-shaped frames as shown in Fig. 3(c), their material and sectional properties are the same as those of

the example bridge; the cable sag to span ratio is 1/10 in elevation, and 8.575/1490 in plane.

(3) Outward-inclined cable system. As shown in Fig. 2(d), the distance of the two main cables is the narrowest at the midpoint of the main span and is gradually expanded towards the tower top. The two towers are both reversed-trapezoid door-shaped frames as shown in Fig. 3(d), their material and sectional properties are the same as those of the example bridge; the cable sag to span ratio is 1/10 in elevation, and 8.575/1490 in plane, the distance of two main cables at tower top is 51.45 m.

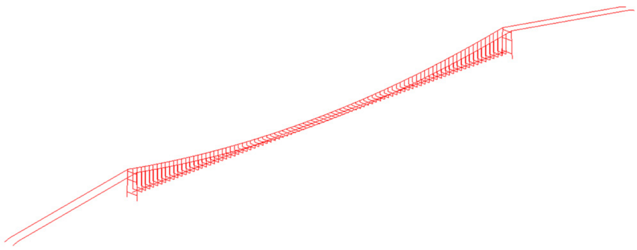

(a) Parallel cable system

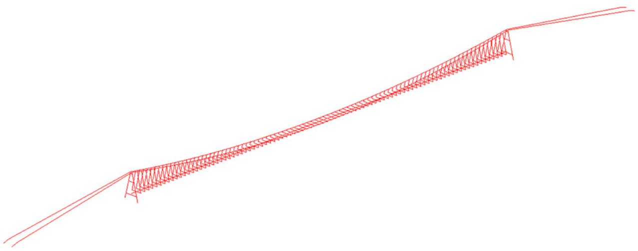

(b) Inward-inclined cable system 1

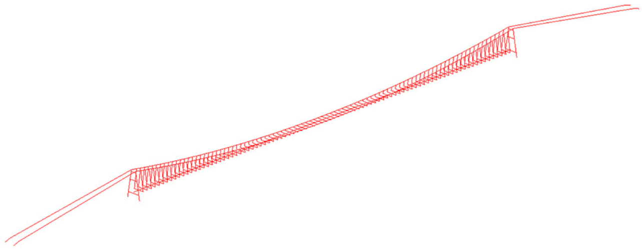

(c) Inward-inclined cable system 2

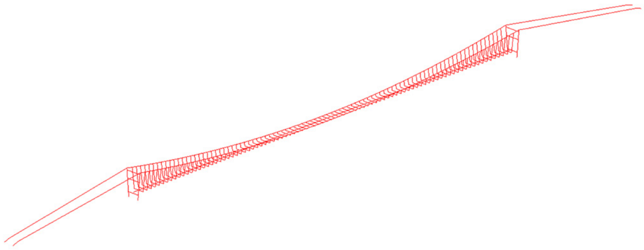

(d) Outward-inclined cable system

Fig.2 3D finite element model of the example bridge and case bridges with different 3D cable systems

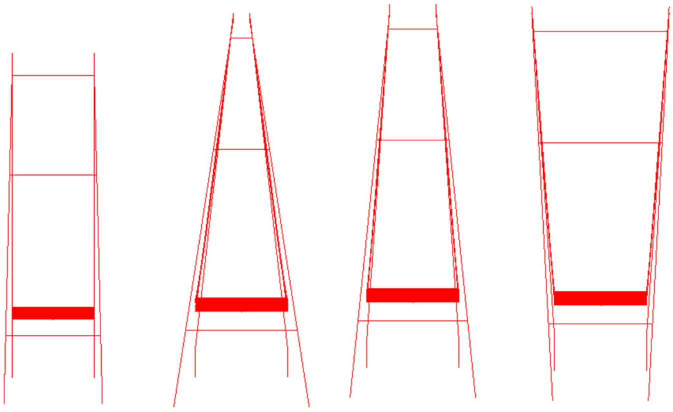

Fig. 3 The front view of the bridges with different cable systems: (a) parallel cable system, (b) inward-inclined cable system 1, (c) inward-inclined cable system 2, (d) outward-inclined cable system

Table 2 The modal properties of bridge deck

Modes	Natural frequency(Hz)				Mode shape
	The example bridge	Inward-inclined cable system 1	Inward-inclined cable system 2	Outward-inclined cable system	
Vertical bending	0.1251	0.1249	0.1250	0.1250	1-S
	0.1005	0.1003	0.1003	0.1004	1-AS
	0.1719	0.1717	0.1718	0.1717	2-S
	0.1880	0.1874	0.1878	0.1878	2-AS
	0.2407	0.2400	0.2404	0.2404	3-S
Lateral bending	0.0496	0.0506	0.0501	0.0493	1-S
	0.1249	0.1257	0.1254	0.1244	1-AS
Torsion	0.2413	0.2675	0.2530	0.2392	1-S
	0.2414	0.2396	0.2399	0.2423	1-AS

Note: The number represents the modal order; S = Symmetric; AS = Anti-symmetric

3. Dynamic characteristics

Firstly, using the numerical method based on the catenary theory, structural geometry and internal force of the example and case bridges with 3D cable system in completion are determined. On the calculated equilibrium position of the four bridges in completion, the first 20 modes of these four bridges are then calculated by the dynamic characteristics finite element analysis(SDCA), in which the subspace iteration method is adopted and structural geometric nonlinearity is also considered(Zhang 2007). Table 2 shows the modal properties of bridge deck. In the following analysis, the bridge is idealized to a 3D finite element model as shown in Fig. 2, in which the bridge deck is idealized to a single-girder model, all the elements are 3D beam elements except the hangers and main cables, which are 3D bar elements with geometrical stiffness, and the connections between the bridge deck and the hangers are modeled by transverse rigid beams. Structural

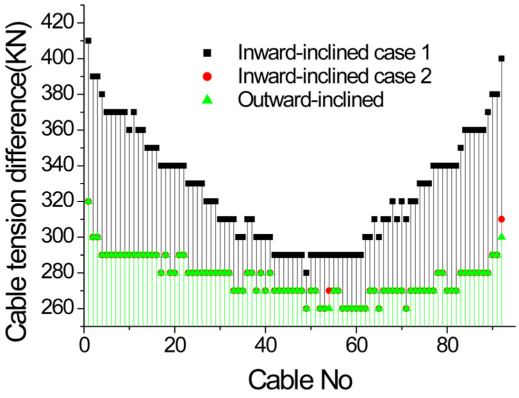

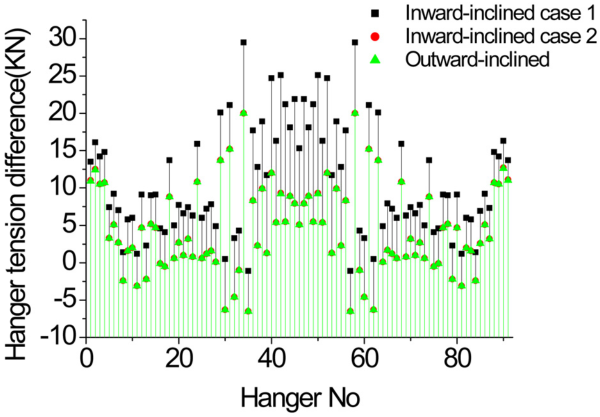

Fig. 4 The tension differences of the main cables and hangers between the case bridges with 3D cable systems and the example bridge

constraint conditions are assumed as follows: at the anchorages and tower bottoms, all the displacements are restricted; at the tower tops, the cable's movements are subordinated to the towers; at the intersections of the bridge deck and tower, the girder's longitudinal movement is restricted at one end, and left free at another end, the vertical and lateral movements of the girder are both subordinated to the towers, the rotation about the longitudinal axis is restricted, and but the rotations about the vertical and lateral axis are both left free.

As found from Table 2, the cable system has almost no influence on the vertical bending frequency. In the case of 3D cable system, the cable sag to span ration in elevation do not change, as observed in Fig. 2, the cable sag to span ration in plane is very little, the cable's tension component in elevation changes little, and consequently the supporting stiffness of main cables for the bridge deck is almost not influenced.

However, the lateral bending and tensional frequencies are influenced by 3D cable system. As compared to the example bridge with parallel cable system, the lateral bending and tensional frequencies increase significantly as the inward-inclined cable system is employed. Therefore, the inward-inclined cable system is confirmed analytically to be effective in strengthening the lateral bending and tensional stiffness. In the case of inward-inclined cable system, there exits lateral tension component in main cables, which provides restraints for the lateral bending and tensional motions of the bridge deck, the lateral bending and tensional stiffness is consequently strengthened. With continual increasing of the cable's lateral sag, as plotted in Fig. 4, the tensions in the hangers and main cables increase simultaneously, especially for the inward-inclined cable system 1, the restraint for lateral bending tensional motions of the bridge deck is further strengthened, which makes the lateral bending and tensional frequencies of the inward-inclined cable system 1 higher than those of the inward-inclined cable system 2.

On the Contrary, as compared to the example bridge with parallel cable system, the lateral bending and tensional frequencies both decrease slightly in the case of outward-inclined cable system. As the deck bends laterally and twists itself, the main cable in one side is tensioned and become tight, and however in another side, it is loosened, and there exists tension difference between the two side main cables. As found in the analysis, the tension difference in the case of outward-inclined cable system is more prominent, and the restraint for the lateral bending and tensional motions decrease consequently, which leads to the reductions of the lateral bending and tensional frequencies.

It can be concluded from the above analysis that a better dynamic characteristic is obtained as the inward-inclined cable system is adopted for suspension bridges.

4. Aerostatic stability

Under the wind attack angles of 0^o and $\pm 3^o$, with the experimentally obtained aerostatic coefficients as shown in Fig. 5 (Xiang and Chen 2000), the aerostatic behaviors of these four bridges are investigated numerically by three-dimensional nonlinear aerostatic analysis(Zhang 2006). In the analysis, the aerostatic drag, lift and twist moment components are applied on the bridge deck; for main cables, hangers and towers, only the aerostatic drag component is applied, and the corresponding drag coefficients is 0.7 for cables and hangers and 2.0 for towers. The evolutions of the deck's displacements at midpoint of main span with wind speed are plotted in Fig. 6. The design wind speed at the bridge deck level is 37.4 m/s(Xiang and Chen 2000), under the design wind speed and wind attack angle of 0^o, the variations of the deck's displacements along the bridge axis are analyzed and plotted in Fig.7.

Under the wind attack angle of -3^o, with increasing of wind speed, the lateral, vertical and tensional displacements all increase nonlinearly, and no sudden changes occur. In the case of $0^o$and $+3^o$ wind attack angels, the lateral displacement increases nonlinearly, and however the vertical and tensional displacements increase slightly at low wind speed, and increase suddenly after a certain wind speed, the bridges start to become aerostatically unstable.

As found in Figs. 6 and 7, under the same wind speed, the inward-inclined cable system 1 has the greatest deformation, then the inward-inclined cable system 2, and the smallest displacements occur for the outward-inclined cable system. Therefore, it can be concluded that the aerostatic instability happens firstly for the inward-inclined cable system 1, and then the inward-inclined cable system 2, and finally the outward-inclined cable system.

It is to be noted that for the inward-inclined case bridge 1, the critical wind speeds of aerostatic instability under the wind attack angles of -3^o, 0^o and $+3^o$ are greater than 80, 90 and 95 m/s respectively, which are all greater than the checking wind speed of aerostatic instability 67.3 m/s, and therefore it is confirmed analytically to be aerostatically stable for these four bridges. However viewed from the aspect of aerostatic stability, the outward-inclined cable system seems more

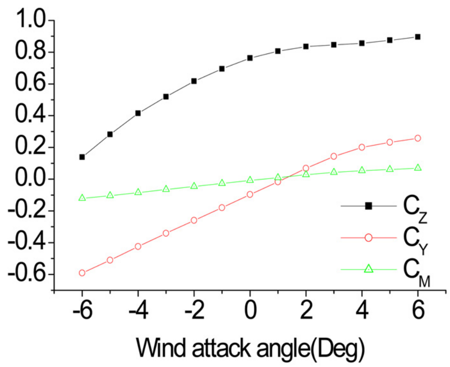

Fig.5 The aerostatic coefficients of the bridge deck

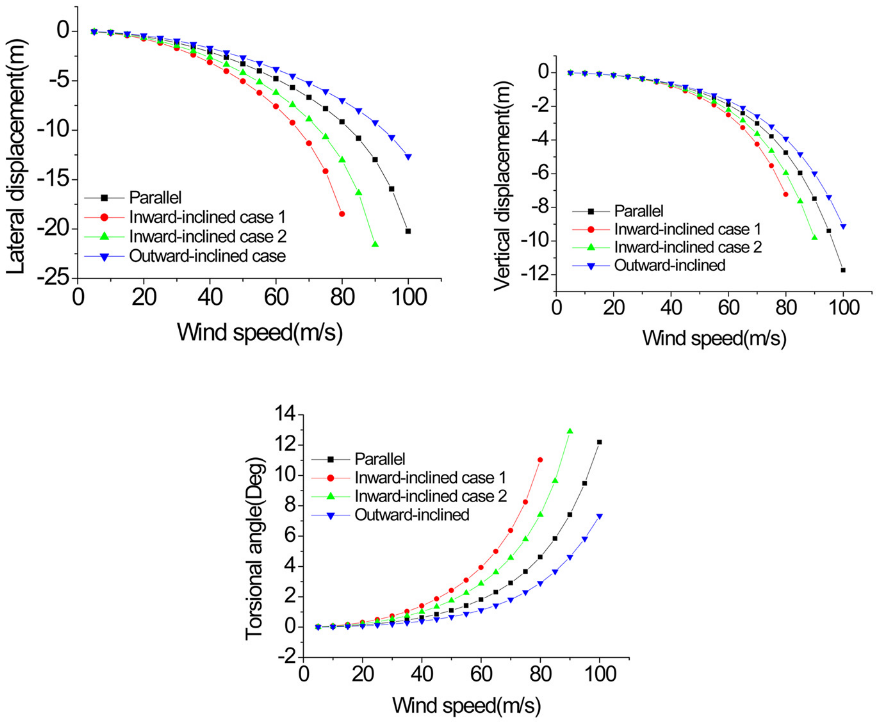

Lateral displacement(m)
Wind speed(m/s)
Parallel
Inward-inclined case 1
Inward-inclined case 2
Outward-inclined case
Vertical displacement(m)
Wind speed(m/s)
Parallel
Inward-inclined case 1
Inward-inclined case 2
Outward-inclined
Torsional angle(Deg)
Wind speed(m/s)
Parallel
Inward-inclined case 1
Inward-inclined case 2
Outward-inclined

(a) -3°

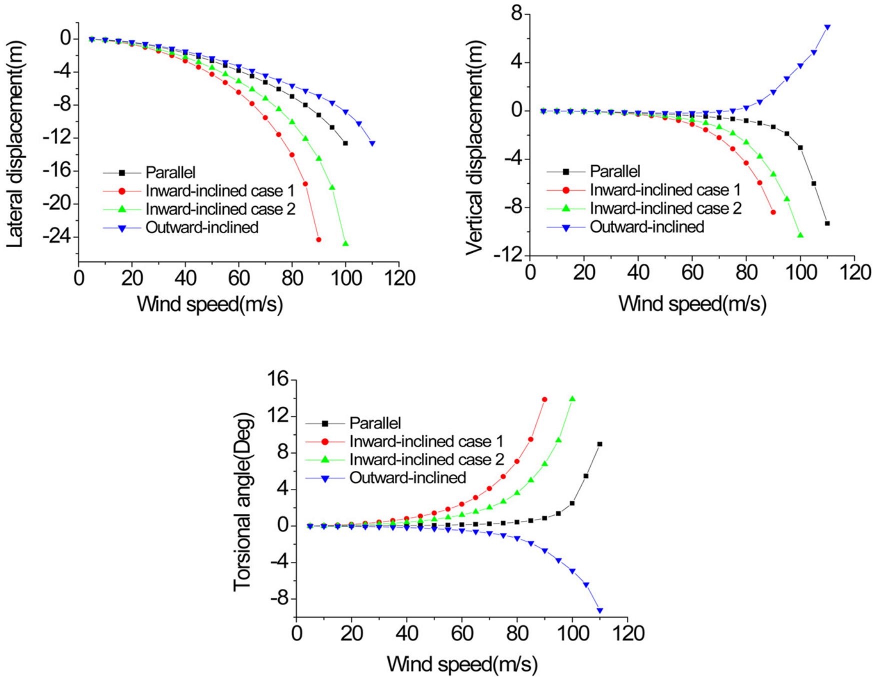

Lateral displacement(m)
Wind speed(m/s)
Parallel
Inward-inclined case 1
Inward-inclined case 2
Outward-inclined
Vertical displacement(m)
Wind speed(m/s)
Parallel
Inward-inclined case 1
Inward-inclined case 2
Outward-inclined
Torsional angle(Deg)
Wind speed(m/s)
Parallel
Inward-inclined case 1
Inward-inclined case 2
Outward-inclined

(b) 0°

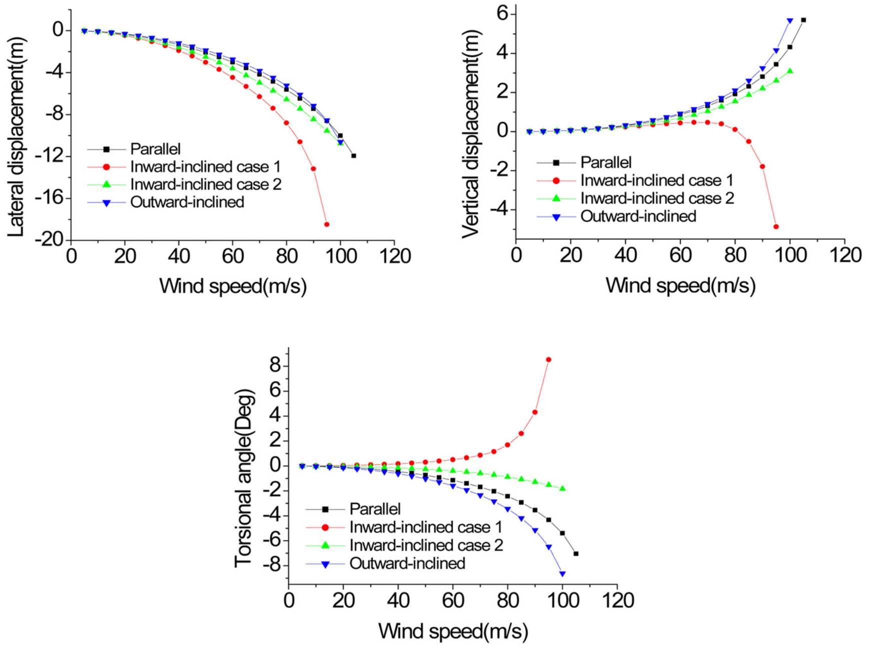

(c) +3^{o}

Fig. 6 Evolutions of the deck's displacements at midpoint of main span with wind speed

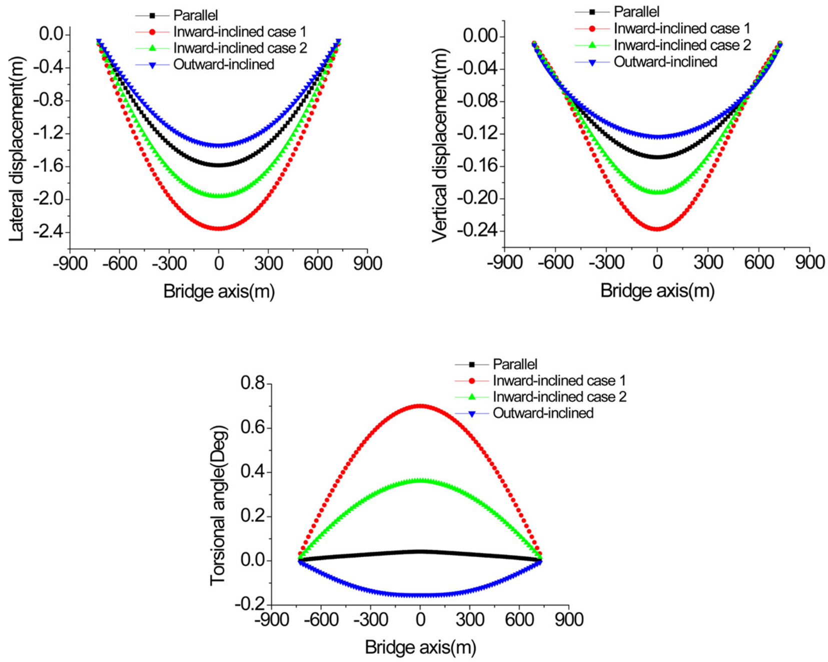

Fig.7 Variations of the deck's displacements along the bridge axis under wind attack angle of 0^{o} and the design wind speed

favorable for long-span suspension bridges.

5. Aerodynamic stability

Under wind attack angles of 0^{o} and $\pm 3^{o}$, with the experimentally obtained flutter derivatives as shown in Fig.8 (Xiang and Chen 2000), aerodynamic stability of these four bridges is investigated numerically by three-dimensional nonlinear aerodynamic stability analysis(BSNAA) (Zhang 2007), and the critical wind speeds of aerodynamic instability are presented in Table 3. In the analysis, the self-excited aerodynamic forces are applied on the bridge deck, and as for the main cables, they are not considered herein. It is because that as found by Zhang(2007), the self-excited aerodynamic forces of main cables have almost no influence on the aerodynamic stability of the bridge. The first 20 modes are involved in the analysis, and the modal damping ratio is taken as 0.5%.

As shown in Table 3, the minimum values of flutter critical speeds for these four bridges are all at the $+3^{o}$ wind angle of attack. Under wind attack angle of $+3^{o}$, except for the outward-inclined cable system, the critical wind speeds of aerodynamic instability of other three bridges are almost the same, and all greater than the flutter checking wind speed 54 m/s(Xiang and Chen 2000), and therefore they are aerodynamically stable. However, under wind attack angles of 0^{o} and -3^{o}, the inward-inclined cable system has better aerodynamic stability than the parallel cable system. The aerodynamic instability of the bridge is found to be a coupled oscillation of the first symmetric vertical bending and the first symmetric torsion. As shown in Table 2, the first symmetric vertical bending frequency is basically not affected by the cable system, and thus the aerodynamic stability of the bridge mainly depends on the first symmetric tensional frequency, and therefore the order of aerodynamic stability for these four bridges is just identical to that of the first symmetric tensional frequency.

In comparison with the aerostatic stability, it is found that the order of aerodynamic stability for these four bridges is just inverse to that of aerostatic stability. However for the example bridge, it is more prone to aerodynamic instability, and considering the whole wind-induced instability, the parallel and inward-inclined cable systems are both favorable for the bridge.

6. Conclusions

In this work, based on the Runyang Highway Bridge over the Yangtze River, three case bridges with different 3D cable systems are designed, structural dynamic characteristics, the aerostatic and aerodynamic stability are investigated numerically by 3D nonlinear aerostatic and aerodynamic analysis, and some important conclusions are drawn as follows:

(1) The cable system has almost no influence on the vertical bending frequency. As compared to the example bridge with parallel cable system, the lateral bending and tensional frequencies increase in the case of inward-inclined cable system, and but decrease under the case of outward-inclined cable system. The bridge with inward-inclined cable system has better dynamic characteristics.

(2) Under the static wind action, the bridge with outward-inclined cable system has the best aerostatic behavior, but under the dynamic wind action, the bridge with either parallel or inward-inclined cable system is more stable aerodynamically.

(3) Considering that the suspension bridge is more prone to aerodynamic instability, and therefore

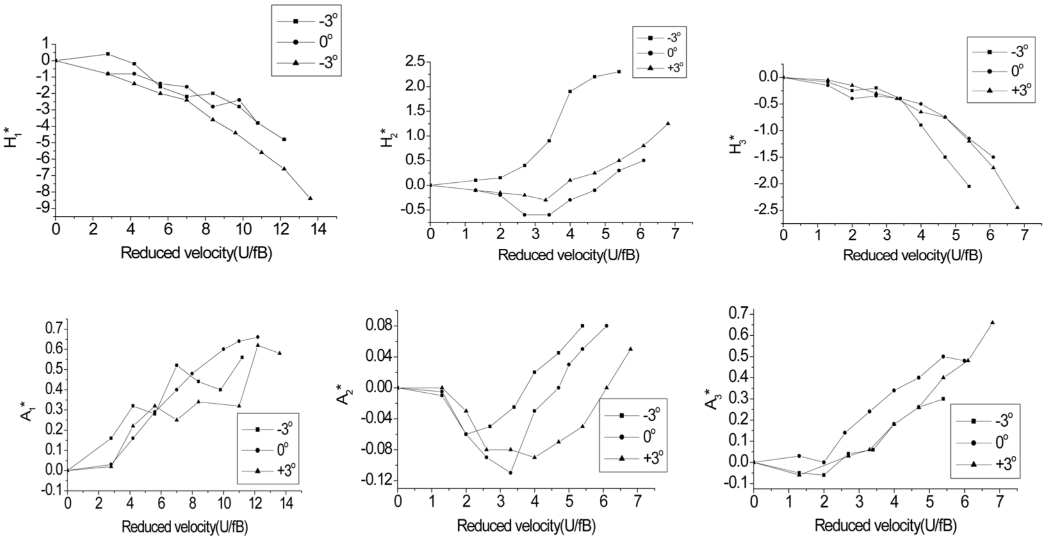

Fig.8 Flutter derivatives at varying angles of wind incidence versus the reduced velocity

Table 3 The critical wind speed of aerodynamic instability (m/s)

Cable system		Parallel	Inward-inclined 1	Inward-inclined 2	Outward-inclined
Wind attack angle	+3°	59.8	59.0	58.5	51.6
	0°	66.0	67.1	68.5	68.8
	-3°	75.7	78.8	79.5	74.9

considering the whole wind-induced instability, the parallel and inward-inclined cable systems are both favorable for long-span suspension bridges.

References

Astiz, M.A.(1996), “Wind related behavior of alternative suspension systems”, *Proceedings of the 15th Congress IABSE,* Copenhagen, Denmark.

Astiz, M.A.(1998), “Flutter stability of very long suspension bridges”, *J. Bridge Eng-ASCE*, **3**(3), 132-139.

Gimsing, N.J.(1997), *Cable-supported bridges-concept and design*, 2nd Ed., John Wiley & Sons Ltd, Chichester, England.

Jensen, P.(2001), “On cable-supported bridges-challenging technical limits”, *Proceedings of the Beauty of Suspended Structures, IABSE Conference,* Soul, Korea.

Kim, H.K., Lee, M.J. and Chang, S.P.(2002), “Non-linear shape-finding analysis of a self-anchored suspension bridge”, *Eng. Struct.*, **24**(12), 1547−1559.

Kubo, Y., Sasaki, M., Nakagiri, H. and Sakata, T.(1995), “Dynamic and flutter characteristics of long-span suspension bridges with 3D cable system”, Bridges into the 21stCentury, Hong Kong.

Kwon, S.D., Changa, S.P., Kimb, Y.S. and Parkc, S.Y.(1995), “Aerodynamic stability of self-anchored double deck suspension bridge”, *J. Wind Eng. Ind. Aerod.*, **54**, 25-34.

Larsen, A. and Astiz, M.A.(1998), “Aeroelastic considerations for the Gibraltar Bridge feasibility study”, Bridge Aerod., Balkema, Rotterdam, 165-173.

Luo, X.H.(2004), Fine analysis of complicated suspension bridge during construction process, Dissertation of Tongji University.

Ochsendorf, A. and Billington, P.(1999), "Self-anchored Suspension Bridges", *J. Bridge Eng.*, ASCE, **4**(3), 151-156.

Osamu, Y., Motoi, O. and Takeo, M.(2004), "Structural characteristics and applicability of four-span suspension bridge", J. Bridge Eng., ASCE, **9**(5), 453-463.

Xiang, H.F. and Ge, Y.J.(2007), "Aerodynamic challenges in span length of suspension bridges", *Frontiers of Architecture and Civil Engineering in China*, **1**(2), 153-162.

Xiang, H.F. and Chen, A.R.(2000), Wind-resistant Research on the Runyang Highway Bridge over the Yangtze River: sectional-model wind tunnel test. The State Key Laboratory for Disaster Reduction in Civil Engineering, Tongji University.

Zhang, X.J.(2006), "Advanced aerostatic analysis of long-span suspension bridges", *J. Zhejiang University SCIENCE A,* **7**(3), 424-429.

Zhang, X.J. (2007), "Influence of some factors on the aerodynamic behavior of long-span suspension bridges", *J. Wind Eng. Ind. Aerod*., **95**(3), 149-164.

Zhou, X.H., Wu, J. and Di, J.(2006), "Mechanical analysis for long-span self-anchored suspension bridges", *J. China Civil Engin.*, **39**(2), 42-45.

CC